Heliyon 10 (2024) e31653

Contents lists available at ScienceDirect

Heliyon

journal homepage: www.cell.com/heliyon

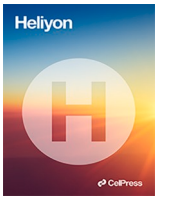

Research article

Methylcellulose improves dissociation quality of adult human primary cardiomyocytes

Xun Shi [a], Rongjia Rao [a], Miaomiao Xu [a], Mengqi Dong [a], Shanshan Feng [a], Yafei Huang [a], Bingying Zhou [a,b,*]

[a] State Key Laboratory of Cardiovascular Disease, Fuwai Hospital, National Center for Cardiovascular Diseases, Chinese Academy of Medical Science and Peking Union Medical College, 167 North Lishi Road, Xicheng District, Beijing, 100037, China
[b] Shenzhen Key Laboratory of Cardiovascular Disease, Fuwai Hospital Chinese Academy of Medical Science, Shenzhen, Shenzhen, China

ARTICLE INFO

Keywords:
Methylcellulose
Human primary cardiomyocytes
Plasma membrane
Ion channel

ABSTRACT

Obtaining high-quality adult human primary cardiomyocytes (hPCM) have been technically challenging due to isolation-induced biochemical and mechanical stress. Building upon a previous tissue slicing-assisted digestion method, we introduced polymers into the digestion solution to reduce mechanical damage to cells. We found that low-viscosity methylcellulose (MC) significantly improved hPCM viability and yield. Mechanistically, it protected cells from membrane damage, which led to decreased apoptosis and mitochondrial reactive oxygen species production. MC also improved the electrophysiological properties of hPCMs by maintaining the density of sodium channels. The effects on cell viability and cell yield effects were not recapitulated by MC of larger viscosities, other cellulose derivatives, nor shear protectants polyethylene glycol and polyvinyl alcohol. Finally, MC also enhanced the isolation efficiency and the culture quality of hPCMs from diseased ventricular myocardium, expanding its potential applications. Our findings showed that the isolation quality of hPCMs can be further improved through the addition of a polymer, rendering hPCMs a more reliable cellular model for cardiac research.

1. Introduction

Cardiovascular diseases (CVDs) are the leading cause of death globally. According to the World Health Organization, CVDs claimed approximately 17.9 million lives, representing 32 % of all global deaths. The urge for better CVD therapeutics has resulted in the development of additional cardiac models that address basic research and drug development needs, one of them being human adult primary cardiomyocytes [1,2].

Adult human primary cardiomyocytes have increasingly become an important *in vitro* model in cardiovascular research due to their outstanding prediction of proarrhythmic risks, mitochondrial toxicity prediction, and delineation of disease mechanisms [3–5]. We have previously reported on the use of a tissue slicing-assisted method for the efficient isolation of human primary cardiomyocytes (hPCMs), a protocol that involves the use of mechanical agitation of the digestion solution to facilitate tissue dissociation [6]. We postulated that this process may inflict hydrodynamic stress on cardiomyocytes, which could affect the viability and other quality measurements of dissociated hPCMs [7,8]. Therefore, reducing such stress may further improve the quality of isolated hPCMs.

Polymer additives have been previously reported to protect cells against fluid mechanical damage [9–12]. Polymers are known to

* Corresponding author. 167 North Lishi Road, Beijing, 100037, China.
E-mail address: zhouby@fuwai.pumc.edu.cn (B. Zhou).

https://doi.org/10.1016/j.heliyon.2024.e31653
Received 5 January 2024; Received in revised form 16 May 2024; Accepted 20 May 2024
Available online 21 May 2024

protect cells via multiple physical and biological mechanisms. Shear stress is a well-established mechanism of cell death in sparged stirred tank bioreactors, while increasing liquid viscosity has been shown to reduce cell damage [13,14]. Air bubbles caused by stirring present an additional layer of stress to cellular membrane [15]. Viscosifiers have been found to reduce cell damage possibly by slowing the movement of bubbles and reducing the wake volume, and are therefore used to control cell death [15]. Cell-to-bubble attachment and resulting bubble burst is another mechanism of cellular damage in stirred bioreactors, which can be effectively dampened by lowering the vapor-liquid interfacial tension of a solution, such as via the addition of polymers [16]. Given the likeness of sparged

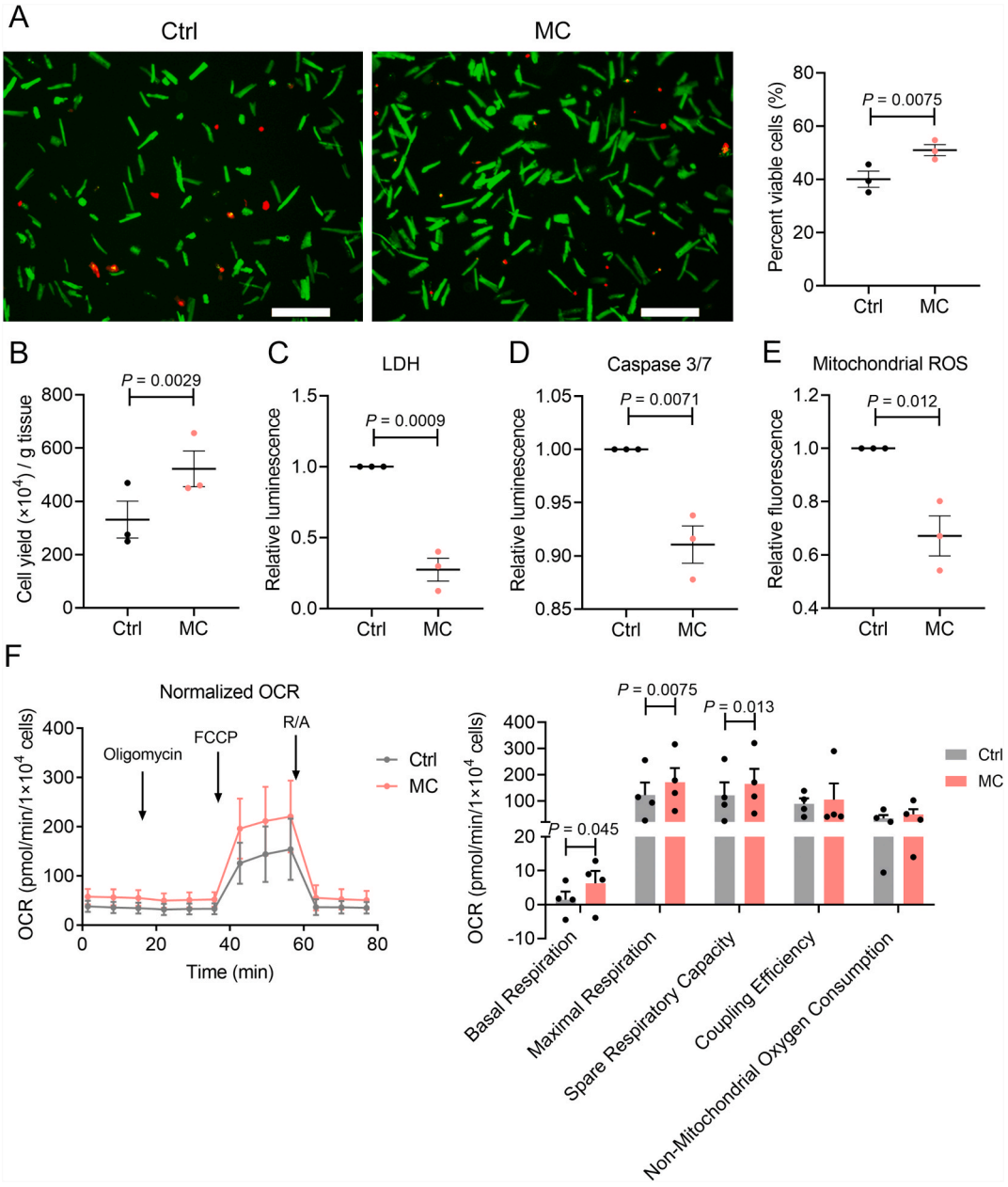

Fig. 1. Methylcellulose improves hPCM isolation quality by preserving membrane integrity. **A**. Cell viability staining of hPCMs isolated using Control (Ctrl) or MC-supplemented isolation buffer (MC). Green, calcein-AM; red, EthD-1. Scale bar = 200 μm. Quantification of cell viability is shown on the right. n = 3 independent experiments. **B**. Quantification of cell yield. n = 3 independent experiments. **C**. LDH measurement for membrane integrity. Readouts were normalized to Ctrl. n = 3 independent experiments. **D**. Caspase 3/7 activity measurement for apoptosis. Readouts were normalized to Ctrl. n = 3 independent experiments. **E**. Mitochondrial ROS detection by MitoSOX Red. Readouts were normalized to Ctrl. n = 3 independent experiments. **F**. Seahorse assay measuring oxygen consumption rate. Right: quantification of basal respiration, maximal respiration, spare respiratory capacity, coupling efficiency, and non-mitochondrial oxygen consumption. n = 4 independent experiments. Data are mean ± SEM. A, B, and F, paired Student's *t*-test. C, D and E, unpaired Student's t-test.

bioreactors and our isolation system, we hypothesized that the addition of agents with such protective properties may enhance the overall quality of isolated cardiomyocytes. Here, we identified MC as an effective polymer to increase cell yield, cell viability, and improve cell morphology and function, through maintaining membrane integrity during hPCM dissociation.

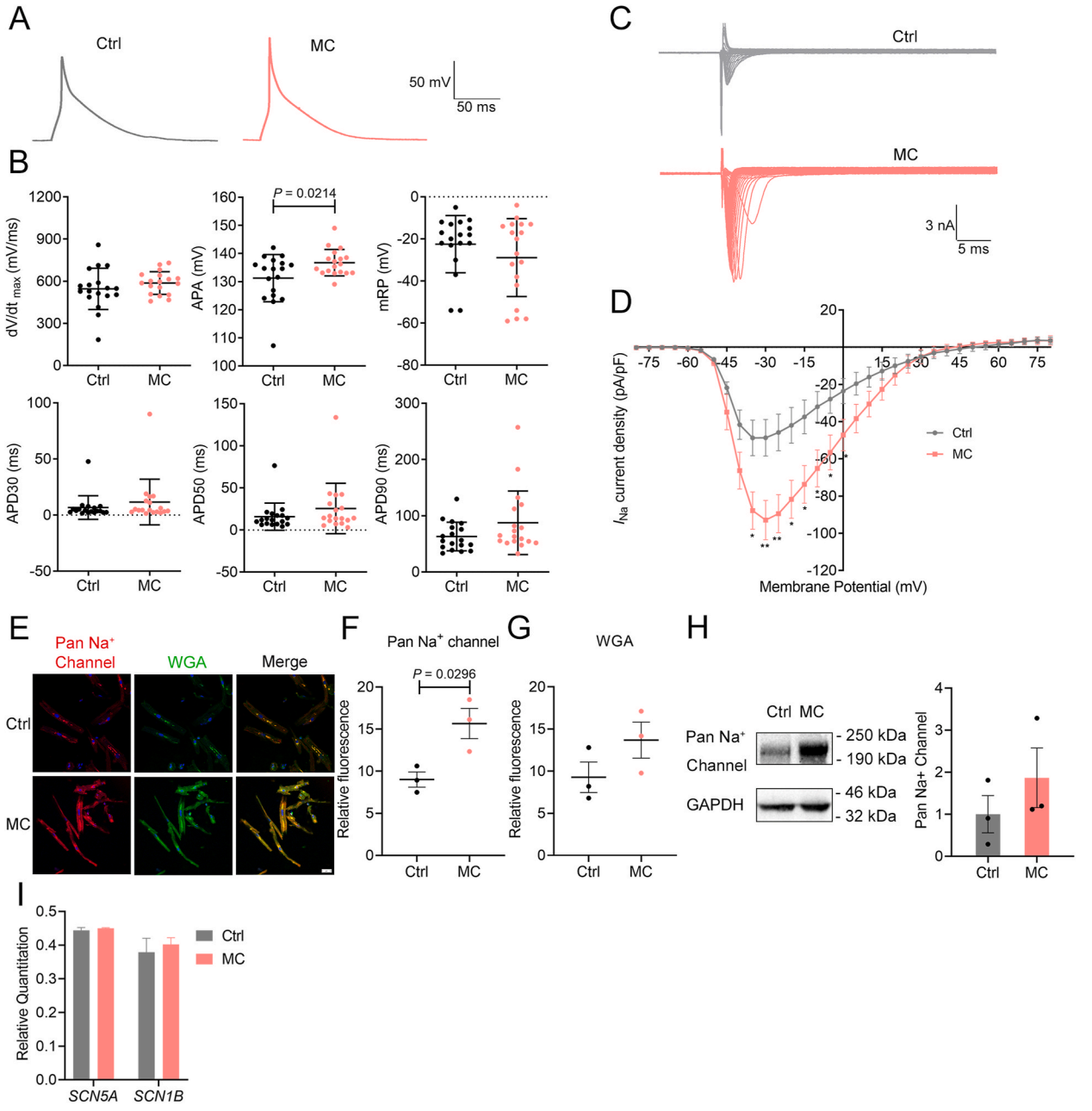

Fig. 2. Methylcellulose preserves sodium channels to improve hPCM electrophysiology. **A-B.** Action potential (AP) recordings of freshly isolated hPCMs. Representative AP tracings are shown (**A**). Quantification of AP parameters (**B**), including rate of membrane depolarization (dV/dt_{max}), action potential amplitude (APA), membrane resting potential (mRP), and action potential durations at 30 % (APD30), 50 % (APD50), and 90 % (APD90), are quantified (bottom). n = 18 cells in Ctrl, and = 18 cells in MC from 3 patients. **C.** Sodium current (I_{Na}) measurement by whole-cell patch clamping. Representative I_{Na} tracings are shown (**C**). **D.** Quantification of the current–voltage relationship. n = 10 cells in Ctrl, and = 9 cells in MC from 4 patients. **E.** Representative immunofluorescence images of pan sodium channel (red), WGA (green), and DAPI (blue) are shown (F). Scale bar = 25 μm. **F-G.** Quantification of (**E**). n = 3 patients, 4–5 images were analyzed per data point. **H.** Representative western blots and densitometric analysis of pan sodium channel expression in control and MC-isolated hPCMs. n = 3 patients. Uncropped gel blots are provided in Figure S1E. **I.** qPCR analysis of *SCN5A* and *SCN1B* expression. n = 3 patients. Data are mean ± SEM. $^{*}P < 0.05$, $^{**}P < 0.01$, Significance was tested using paired Student's *t*-test.

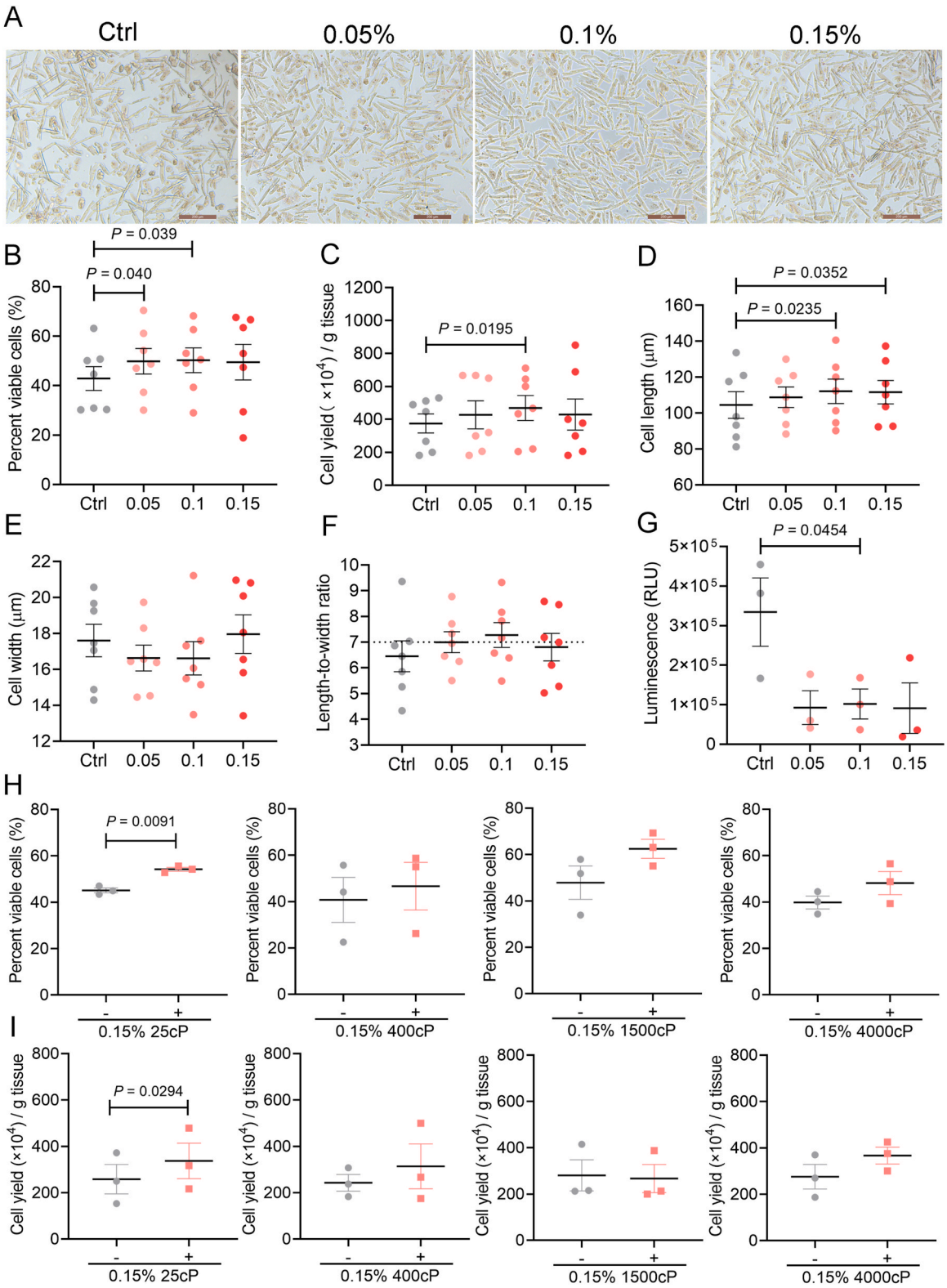

Fig. 3. Optimal concentration and molecular weight of MC for hPCM isolation. **A.** Representative bright field images of freshly isolated hPCMs using different concentrations of MC. Green, calcein-AM; red, EthD-1. Scale bar = 200 μm. **B.** Quantification of cell viability. n = 7 independent experiments. **C.** Quantification of cell yield. n = 7 independent experiments. **D-F.** Quantification of cell shape parameters, including cell length (D), cell width (E), and length-to-width ratio (F). n = 350 cells each group, analyzed from 7 patients (50 cells per treatment group per patient). **G.** LDH

measurement for membrane integrity. n = 3 independent experiments. **H–I.** Quantification of cell viability (H) and cell yield (I) of hPCMs isolated using Ctrl or MC of different viscosities (25, 400, 1500, and 4000 cP). n = 3 independent experiments. Data are mean ± SEM. Significance was tested using paired Student's *t*-test.

2. Results

2.1. Methylcellulose improves hPCM isolation quality by preserving membrane integrity

First, we set out to test whether the use of methylcellulose (MC) during isolation affected the viability and yield of isolated human primary cardiomyocytes (hPCMs). At a concentration of 0.25 %, MC (viscosity 15 cP, cP) significantly enhanced viability compared to control (Ctrl) (Ctrl vs MC, 40.04 ± 3.041 % vs 50.95 ± 2.091 %, $P < 0.01$) (Fig. 1A). Accordingly, MC also raised the cell yield from 3.31 ± 0.69 × 10^6 cells in control to 5.22 ± 0.67 × 10^6 cells per gram of tissue in MC ($P < 0.01$) (Fig. 1B). To understand how MC exerted its protective effects, we measured lactate dehydrogenase (LDH) release, and observed marked reduction of LDH release upon the use of MC, suggesting that MC protected hPCMs from cell membrane rupture and necrosis ($P < 0.001$, Fig. 1C). In addition, MC also appeared to reduce hPCM apoptosis, as measured by caspase 3/7 activity ($P < 0.01$, Fig. 1D). Mitochondrial oxidative stress in hPCMs was also attenuated upon the addition of MC ($P < 0.05$, Fig. 1E). Furthermore, MC-isolated cells exhibited significantly increased basal respiration ($P < 0.05$), maximal respiration ($P < 0.01$), and spare respiratory capacity ($P < 0.05$) compared to control cells, suggesting that mitochondrial function was better preserved (Fig. 1F). As expected, MC did not alter cardiomyocyte marker gene expression of isolated hPCMs (Figure S1A).

2.2. Methylcellulose preserves sodium channels to improve hPCM electrophysiology

Given that MC preserved hPCM membrane integrity, we examined whether it had any effect on hPCM electrophysiology, which is highly contingent on ion channels on the plasma membrane. While action potential (AP) durations and the rate of membrane depolarization (dV/dt_{max}) only showed increasing trends, action potential amplitudes (APA) were significantly greater in MC compared to control (Ctrl vs MC, 131.3 ± 1.98 mV vs 136.7 ± 1.108 mV, $P < 0.05$) (Fig. 2A and B). The resting potential (mRP) also exhibited a trend towards greater negativity, which failed to reach statistical significance (Fig. 2B). These observations indicated that membrane proteins were better preserved in the MC group, particularly sodium channels, which are the major determinants of APA. Consistently, Na^+ currents (I_{Na}) were markedly increased in MC-isolated hPCMs compared to control (Fig. 2C and D), while other parameters, including activation, inactivation and recovery dynamics of I_{Na}, remained unaltered (Figure S1B-D). The enhancement of I_{Na} led us to determine whether it arose from increased sodium channel densities on the cell surface. Immunofluorescence staining of sodium channels revealed significant 1.74-fold increase ($P < 0.05$) in the mean fluorescence intensities in MC compared to control, suggesting better preservation of sodium channel abundance (Fig. 2E and F). Wheat germ agglutin (WGA), which binds cell surface glycans, and thus also an indicator of membrane integrity, also showed an increasing trend, indicating reduced destruction of the plasma membrane (Fig. 2G). In accordance with these data, western blotting analysis also revealed an increasing trend in pan sodium channel expression in the MC group (Fig. 2H and S1E). *SCN5A* encodes the predominant cardiac sodium channel α subunit Nav1.5, while *SCN1B* encodes the β1 subunit. MC did not induce the expression of *SCN5A* or *SCN1B* transcripts, suggesting that the increase in sodium channel expression was not due to enhanced transcription (Fig. 2I).

In an effort to understand how MC might have produced such effects, we tested the changes in some physical properties upon the addition of MC into the solution. MC reduced surface tension and enhanced fluid viscosity of the isolation buffer, potentially explaining its protective effects on the plasma membrane (Figure S1F-G). Taken together, these findings suggest that MC protected hPCMs from isolation stress, resulting in enhanced cardiomyocyte function.

2.3. Optimal concentration and molecular weight of MC for hPCM isolation

Next, we sought to determine the optimal working concentration for MC. First, we compared 0.25 % to a higher concentration (0.5 %). However, the increases in cell yield and cell viability were absent using 0.5 % MC (Figure S1H). Therefore, we lowered MC concentration stepwise, and observed gradually increasing cell yield. A concentration of 0.15 % MC showed significant improvement in cell yield (Figure S1I). Since the increase in cell yield has still not reached an inflection point, we tried further reducing MC concentration. Both 0.05 % and 0.1 % MC enhanced hPCM isolation viability (control vs 0.05 % vs 0.1 %, 42.86 ± 4.852 % vs 49.85 ± 5.182 % vs 50.27 ± 5.017 %), while only 0.1 % showed significantly enhancement of cell yield (control vs 0.1 %, 3.75 ± 0.58 × 10^6 vs 4.69 ± 0.76 × 10^6 cells per gram) (Fig. 3A–C). Cell shape is also considered an important measure of cell status and relaxation state, and the aspect ratio of a typical healthy cardiomyocyte at diastole is approximately 7:1 [17]. At 0.1 % and 0.15 %, MC-isolated cells had significantly greater cell lengths, while all concentrations produced cells with aspect ratios closer to 7:1 than control (Fig. 3D–F). Of these concentrations, 0.1 % MC also provided superior protection of membrane integrity ($P < 0.05$, Fig. 3G).

To determine whether the protective effect of MC was dependent on polymer size (i.e., molecular weight), we tested MC of various viscosities, i.e., 25, 400, 1500, and 4000 cP. Viscosity is a function of, and therefore proportional to, the molecular weight for polymers like MC [18]. Of all formulations, only MC-25 (i.e., MC with a viscosity of 25 cP) demonstrated significantly increased cell viability, and cell yield (Fig. 3H and I). These findings indicated that MC of lower viscosities (15–25 cP) had greater protective potential than those of higher viscosities (400–4000 cP).

2.4. Other cellulose derivatives do not recapitulate the protective effects of MC

To determine whether other cellulose derivatives were also capable of improving both cell viability and cell yield, we selected hydroxyethyl cellulose (HEC, hydrophilic side chain), hydroxypropyl cellulose (HPC, hydrophilic side chain) and hydroxypropyl methylcellulose (HPMC, both hydrophilic and hydrophobic side chains), which are also non-ionic cellulose ethers commonly used in pharmaceutical preparations [19]. However, none of these polymers, at varying molecular sizes, displayed protection from physical stress, evidenced by lack of overall improvement in cell viability (Fig. 4A) and cell yield (Fig. 4B). These observations indicate that other cellulose derivatives fail to produce similar protective effects than MC, suggesting that hydrophilic side chains (hydroxyethyl and hydroxypropyl groups) may interfere with membrane protection.

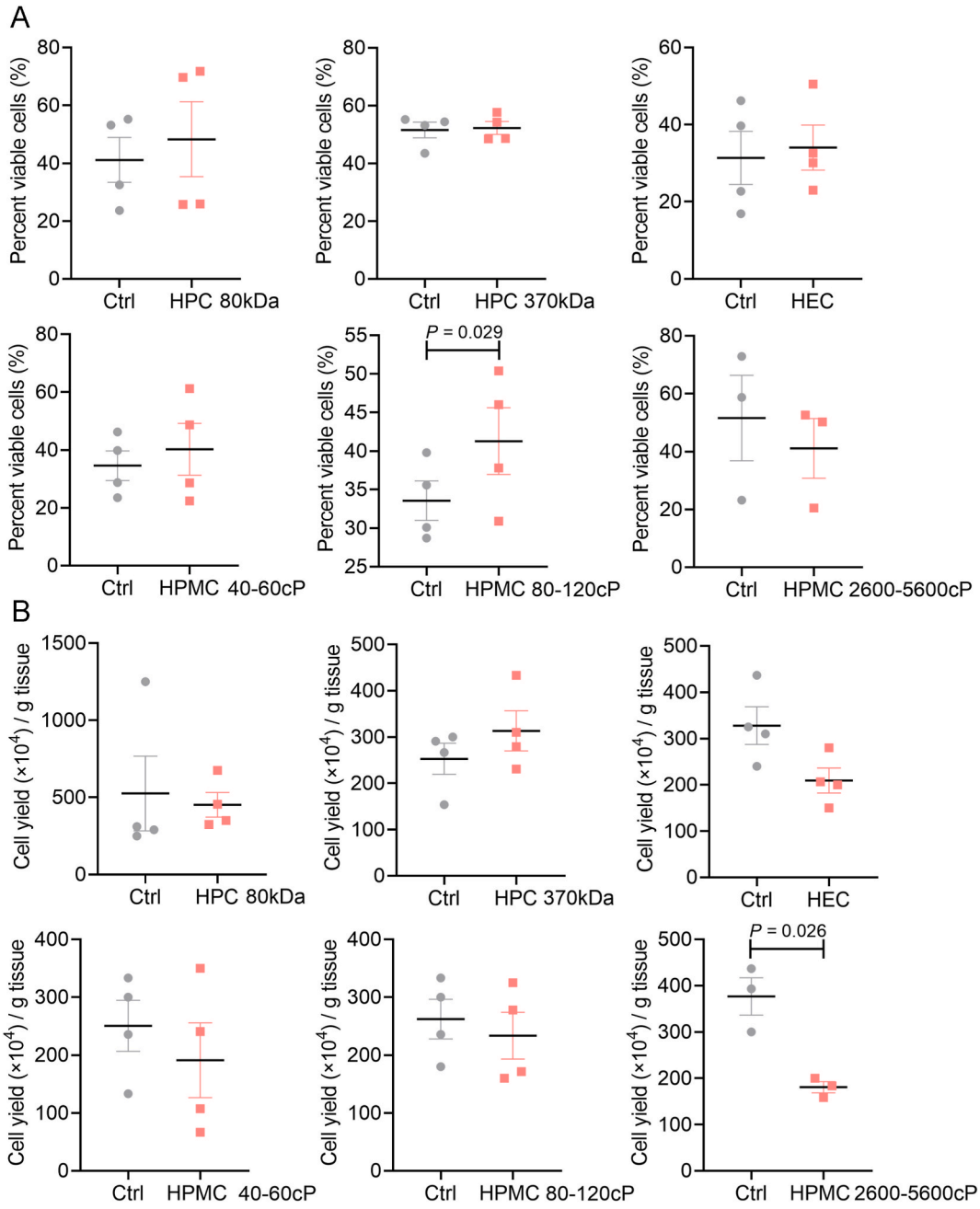

Fig. 4. Cellulose derivatives do not recapitulate the protective effects of MC. **A-B**. Quantification of cell viability (**A**) and cell yield (**B**) of hPCMs isolated using Ctrl or cellulose derivatives (HPC, HEC, HPMC) of different molecular weights or viscosities. n = 3 or 4 independent experiments. Data are mean ± SEM. Significance was tested using paired Student's *t*-test.

2.5. Shear protectants PEG and PVA fail to provide sufficient isolation protection

To this end, we further selected other shear protectants, including polyethylene glycol (PEG), and polyvinyl alcohol (PVA), which have been previously used in bioreactors, to assess their ability to reduce physical damage to hPCMs during isolation [9–11]. First, we compared the effectiveness of 0.1 % PEG (8 kDa) and 0.2 % PVA (13–23 kDa) during the isolation of hPCMs. Interestingly, 0.1 % PEG and 0.2 % PVA both significantly enhanced cell yield, but failed to improve cell viability over control (Fig. 5A and B). Measurement of membrane integrity revealed that while PEG failed to significantly reduce membrane damage ($P = 0.0663$), PVA effectively protected the cellular membrane (55.85 % decrease in LDH release, $P = 0.0474$) (Fig. 5C). However, MC resulted in even greater preservation of the plasma membrane (74.47 % decrease in LDH release, $P = 0.0329$) (Fig. 5C).

We also evaluated other concentrations of PEG and PVA to determine their optimal concentrations for hPCM isolation. PEG concentrations lower or higher than 0.1 % (i.e., 0.5 % and 0.2 %) did not confer greater protection than 0.1 %, as determined by cell viability and cell yield assessment (Figure S2A). In the same vein, PVA concentrations lower or higher than 0.2 % (i.e., 0.1 % and 0.4 %) also exhibited less protective potential than 0.2 % (Figure S2B). In the same vein, we also screened PEG and PVA of different molecular weights. While both PEG-1000 (1 kDa) and PEG-4000 (4 kDa) improved cell yield over control, neither enhanced cell viability (Fig. 5D and E). PVA polymers of other molecular weights (i.e., 9–10, 31–50, and 85–12.4 kDa) also failed to exert a pronounced effect on hPCM isolation (Fig. 5D and E). These observations suggest that low molecular weight MC (15–25 cP) outperforms MC of other molecular weights, as well as all sizes and concentrations of PEG and PVA.

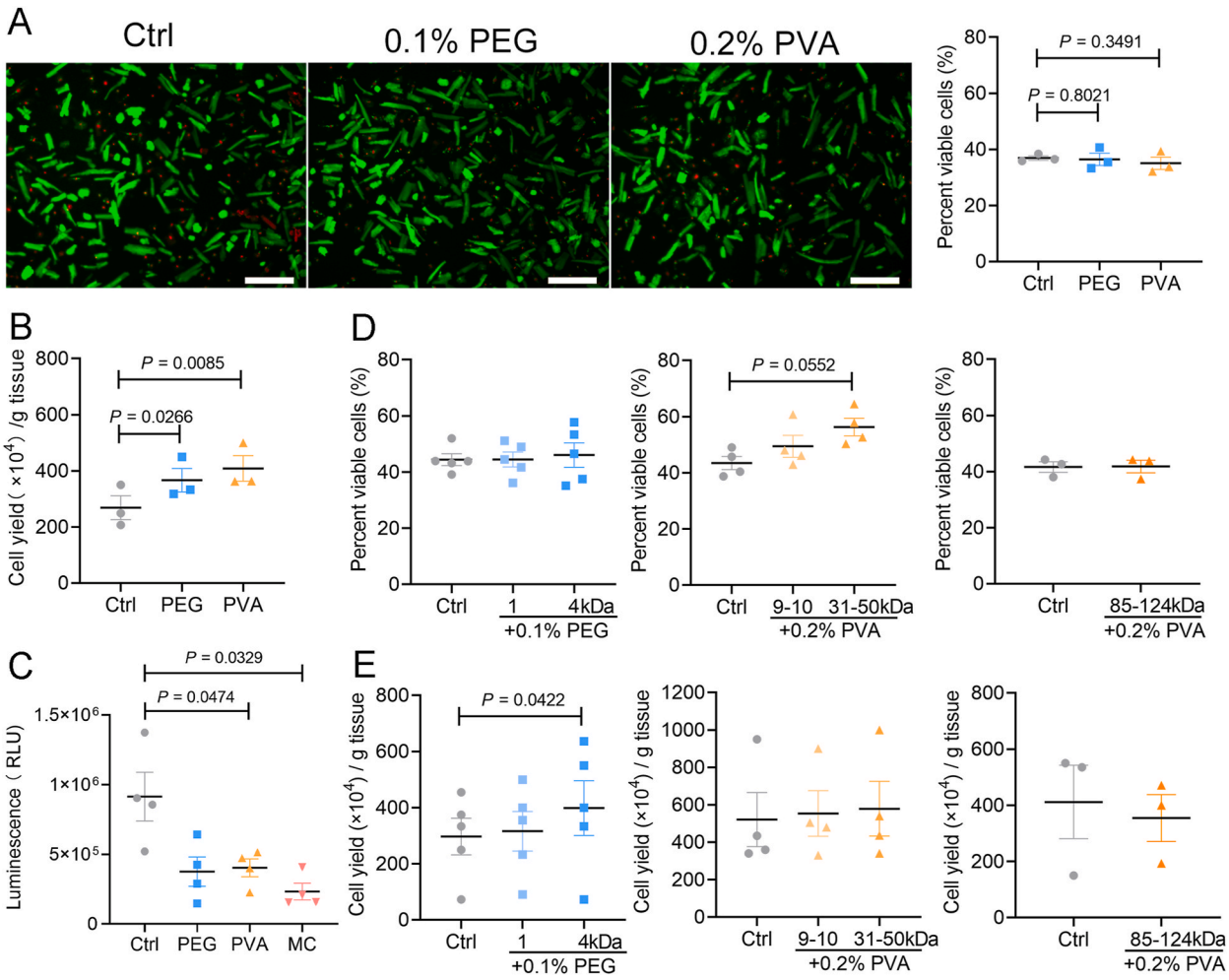

Fig. 5. Shear protectants PEG and PVA fail to provide sufficient isolation protection. **A.** Cell viability staining of hPCMs isolated using Control (Ctrl), PEG- or PVA-supplemented isolation buffer. Green, calcein-AM; red, EthD-1. Scale bar = 200 μm. Quantification of cell viability is shown on the right. n = 3 independent experiments. **B.** Quantification of cell yield. n = 3 independent experiments. **C.** LDH measurement for membrane integrity. n = 4 independent experiments. **D-E.** Quantification of cell viability (D) and cell yield (E) of hPCMs isolated using Ctrl, PEG or PVA of different molecular weights. n = 3 or 4 independent experiments. Data are mean ± SEM. Significance was tested using paired Student's *t*-test.

2.6. MC enables high-quality isolation and culture of diseased ventricular hPCMs

Compared to atrial hPCMs, ventricular hPCMs are more difficult to isolate, particularly ones from diseased cardiac tissues. To test the robustness of our method in enhancing the performance of hPCM isolation, we isolated cells from the left ventricular free walls of 7 end-stage heart failure patients who underwent heart transplantation. The addition of MC significantly enhanced cell viability and cell yield (Fig. 6A and B). Consistently, cell membrane integrity was better preserved in the MC group (Fig. 6C). Finally, we asked whether this protective effect extended beyond the isolation procedure, and exerted long-lasting influence over hPCM quality. To this end, we isolated hPCMs using both methods (Ctrl and MC), and cultured them under identical conditions (without MC) for 7 days to observe changes in cell shape. The maintenance of cell shape was slightly more pronounced in the MC group. By day 3, the average lengths of hPCMs in control and MC groups were 54.97 ± 3.011 μm and 58.28 ± 1.027 μm, respectively. By day 7, cell lengths in the MC group were also 5.06 % larger than those in the control group (Fig. 6D and E). The widths of hPCMs in the control group significantly decreased during culture, whereas those in the MC group did not reduce significantly (Fig. 6D and E). Therefore, MC-mediated protection of the cell membrane lasted through *in vitro* culture, providing lasting maintenance of cellular morphology.

3. Discussion

The isolation of adult cardiomyocytes had been a technical challenge due to the rigid structure, the tight interconnections, and the sensitivity to hypoxic injury of adult cells. Previous techniques relied on biochemical or biological protection of cells during isolation, such as by minimizing hypoxic damage, avoiding energy deprivation, and preventing calcium paradox. Our study is the first to employ

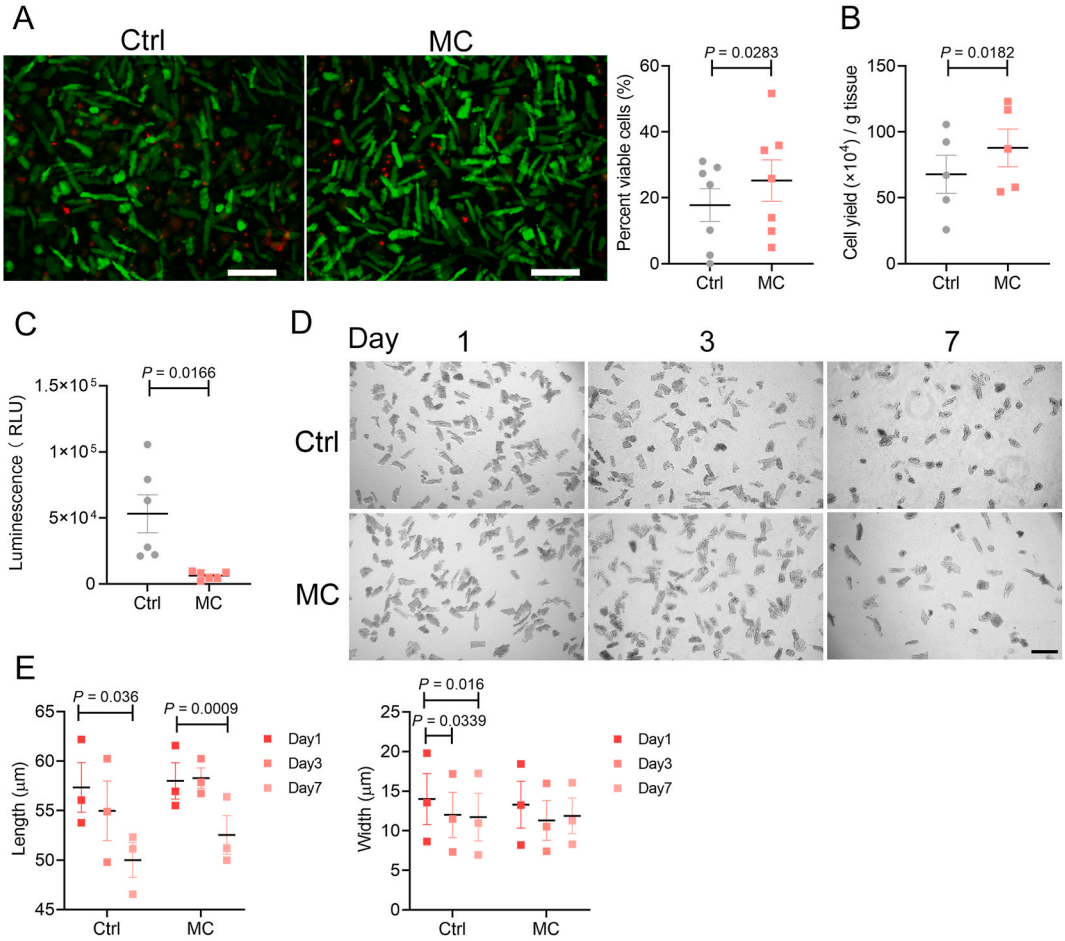

Fig. 6. MC enables high-quality isolation and culture of diseased ventricular hPCMs. **A.** Cell viability staining of hPCMs from the left ventricular wall of end-stage heart failure patients isolated using Control (Ctrl), 0.1 % MC-supplemented isolation buffer. Green, calcein-AM; red, EthD-1. Scale bar = 200 μm. Quantification of cell viability is shown on the right. n = 7 independent experiments. **B.** Quantification of cell yield. n = 5 independent experiments. **C.** LDH measurement for membrane integrity. n = 6 independent experiments. **D.** In vitro culture of diseased left ventricular hPCMs. Representative images of cultured hPCMs on days 1, 3 and 7. Scale bar = 100 μm. **E.** Cell shape measurements of cells from (D). n = 3 independent experiments. Data are mean ± SEM. A-E, paired Student's *t*-test.

polymers in the use of adult cardiomyocyte isolation, controlling for physical damage to cells. We uncovered the ability of MC to protect from membrane injury during hPCM isolation. MC is the simplest cellulose derivative, produced by reacting methyl chloride and alkali cellulose [20]. It generally contains 27.58%–31.5 % of methoxy groups, which give the compound good surface properties [21]. It is one of the most important commercial cellulose ethers and has been used in a variety of industrial applications, as well as in clinical use as a laxative [22,23]. Currently, the application of MC in the biomedical research arena has mainly focused on its use in hydrogels [24]. Our study extends its use as a cell membrane protectant in the establishment of a cellular model for cardiac research. In a previous report, poloxamer 188, a nonionic linear copolymer, has been reported to protect adult rat cardiomyocytes from hypoxia-reoxynation injury through membrane stabilization [25]. However, the exact mechanisms underlying this protective effect remain unclear. Polymers are known to reduce surface tension, shear stress, cell-bubble attachment, and participate in membrane sealing [13–16,26]. It would be interesting to elucidate the detailed mechanisms by which MC maintained membrane integrity, and explore additional scenarios for MC application.

It was interesting that MC of higher molecular weights failed to exhibit similar protection. It is possible that larger molecules could interfere with enzyme exposure and thus reduce overall digestion efficiency. Other cellulose derivatives also failed to produce similar outcomes as MC, possibly due to different hydrophobicity profiles [27]. Hydrophobic methyl groups introduced onto a hydrophilic cellulose backbone may have provided the appropriate surface properties required for membrane protection, while substitution by hydrophilic groups may have reduced the interactions of polymers with the lipid bilayer of the plasma membrane. PEG and PVA both afforded membrane protection, but to a lower degree than MC, which might explain the lack of increase in the resulting cell viability. Thus, determining the optimal surface properties suited for membrane protection may lead to the discovery and synthesis of even better protectants.

4. Methods

4.1. Human samples

The study was approved by the Ethics Committee of Fuwai Hospital, Chinese Academy of Medical Sciences, and Peking Union Medical University, and conducted according to the Declaration of Helsinki (2021-1533). Written informed consent was obtained from all patients. For minors involved in this study (under age 18), written informed consent was obtained from the guardian. A total of 100 patients (male 78, female 22, age range 12–78) were included in this study. Specimens of the left atrial appendage or left ventricle were used for the isolation of cardiomyocytes. Detailed patient and tissue information is listed in the Supplemental Materials (Table S1. Patient information).

4.2. Polymers

All polymers used in this study were purchased from Sigma. Detailed information regarding each polymer is listed in the Supplemental Materials (Table S2. Polymer information). Polymer stock solutions (concentrations listed in Table S2) were prepared by adding them to deionized water (preheated to 50–60 °C), and allowed to swell for 12 h before stirring for another 24 h at the same temperature. Stock solutions were added at the desired working concentrations in the Tyrode's solution prior to isolation of cardiomyocytes.

4.3. Isolation and culture of adult human primary cardiomyocytes

The isolation and culture of human primary CMs were performed as previously described [6] with slight modifications. In brief, human myocardial tissue were cut into slices using a vibrating microtome. Tissue mass was measured by harvesting all cut slices, briefly draining them in a cell strainer, and transferring them into a dry 6-cm dish for weighing. This measurement was used for the calculation of cell yield. Afterwards, tissue slices were immersed again in University of Wisconsin solution (Belzer, CHD120419), cut into smaller pieces using scissors, and transferred to a calcium-free Tyrode's solution (126 mM NaCl, 4.4 mM KCl, 5 mM $MgCl_2{\cdot}6H_2O$, 5 mM NaH_2PO_4, 5 mM HEPES, 22 mM glucose, 20 mM taurine, 5 mM creatine, 5 mM sodium pyruvate), containing 10 μM (−)-blebbistatin (Selleck, S7099), 1.2 U/ml protease XXIV (Sigma, P8038) and 250 U/ml Type I collagenase (Worthington, LS004196) for first-step digestion. For isolation groups containing polymers, polymer stock solutions were prepared as described in the "Polymers" section, and added into the digestion solution at the desired concentration. After 50 min in a 37 °C shaking water bath, the tissue was transferred to a fresh digestive solution that does not contain proteases for subsequent digestion steps. Rod-shaped CMs were collected by gentle centrifugation (100×*g*, 3 min, 4 °C). Cell yield was calculated by dividing the absolute cell count by tissue weight. Calcium concentration was gradually restored to 1.8 mM prior to culture in MEM (HEPES, GlutaMAX™, Gibco, 42360099) supplemented with 1 % BSA (MP Bio, 0219989680), 100 U/ml P/S (Gibco, 20012050), 100 μg/ml Primocin (InvivoGen, ant-pm-2) and 10 μM (−)-blebbistatin.

4.4. Cell viability and cell size assessment

Cell viability staining was performed using the LIVE/DEAD™ Viability/Cytotoxicity Kit (ThermoFisher, L3224), following the manufacturer's instructions. Briefly, cells were stained using calcein-CM and EthD-1 for 10 min in the dark. Then, supernatant was removed by gentle centrifugation (100×*g*, 1 min, RT). Cells were washed once with Tyrode's solution, before imaging on a microscope

(Leica, DMI4000B). Cell viability was quantified by manual counting of green (live) versus red (dead) cells from 6 random independent images per group in ImageJ (v1.8.0). Cell viability was calculated as follows: Cell viability = number of live cells/total cell number × 100 %. Of note, round cells with bright green fluorescent were considered apoptotic, and thus excluded from live cell count.Cell size measurements were also performed using ImageJ (v1.8.0).

4.5. Lactate dehydrogenase (LDH) assay

LDH measurements were performed using the LDH-Glo™ Cytotoxicity Assay kit (Promega, J2380) according to the manufacturer's instructions. For each group, 3×10^4 cells were used for LDH measurement. The total volume of cellular suspension containing 3×10^4 cells were recorded as V. Cellular supernatant was added in triplicate into clear-bottom white 96-well plates (50 μl/well). The LDH detection reagent was added at 1:1 (v/v) ratio into the wells. The reaction was incubated in the dark for 1 h at RT, before luminescence values were measured using a plate reader (BioTek, Synergy LX). The remaining cell pellet was resuspended using 270 μl of Tyrode's solution, to which 30 μl of Prestoblue™ HS Cell Viability Reagent (ThermoFisher, P50201) was added and mixed. This cell suspension was added to a 96-well plate in triplicate wells (100 μl per well), incubated for 10 min at 37 °C. The optical density (OD) was measured using the plate reader. LDH luminescence was calculated using equation (1):

$$\text{Lum (RLU)} = \frac{\text{Lum(Average)} \times \text{V}}{50\ \mu\text{l} \times \text{OD}} \tag{1}$$

4.6. Caspase 3/7 activity assay

Caspase activity measurements were performed using Caspase-Glo® 3/7 Assay System (Promega, G8090) according to the manufacturer's instructions. For each group, 3×10^4 cells were used. Cell suspension volumes were normalized to 300 μl per group using Tyrode's solution, and mixed gently. The resulting cell suspension was added in triplicate into clear-bottom white 96-well plates (100 μl/well). Then, a substrate-buffer mix was added at 1:1 (v/v) ratio into the wells. The reaction was mixed on a plate reader at 300–500 rpm for 30 s, and incubated in the dark for 0.5–1 h at RT, before luminescence was measured. Assay readouts were normalized to cell number as measured by the Prestoblue™ reagent (i.e., OD). Caspase 3/7 luminescence was calculated using equation (2):

$$\text{Lum (RLU)} = \frac{\text{Lum(Average)}}{\text{OD}} \tag{2}$$

4.7. Measurement of mitochondrial ROS

Mitochondrial ROS was measured using the MitoSOX™ Red reagent (Invitrogen, M36008). Briefly, 1×10^4 cells per group were seeded into clear-bottom black 96-well plates, and incubated for 1 h before analysis. A working solution of 5 μM MitoSOX Red reagent was prepared by dilution in HBSS (Gibco,14025092). The working solution was added to cells, and incubated for 10 min at 37 °C. After incubation, cells were gently washed with 37 °C HBSS. Fluorescence measurements were taken on a plate reader (BioTek, Synergy LX).

4.8. Measurement of oxygen consumption rate

Measurement of oxygen consumption rate (OCR) was conducted on a Seahorse XF Pro Analyzer (Agilent, USA). Following isolation, cells were seeded at a density of 5–8 × 10^4 cells per well in Seahorse 96-well XF cell culture microplates (Agilent, 103794-100), and incubated at 37 °C for 1 h in a humidified incubator with 5 % CO_2. Following cell number determination using the Prestoblue™ HS Cell Viability Reagent (ThermoFisher, P50201), the culture medium was replaced with a detection medium containing XF DMEM Medium (Agilent), 10 mM glucose, 1 mM sodium pyruvate, and 2 mM L-glutamine and incubated for 45–60 min prior to the assay at 37 °C in a non-CO_2 incubator. A real-time measurement of OCR was performed followed by the sequential injections of 2 μM oligomycin, 1 μM FCCP, and a mixture of rotenone and antimycin A (0.5 μM). OCR values were analyzed using the Wave Pro software and normalized to cell numbers acquired prior to the assay.

4.9. Whole-cell patch clamping

The electrophysiological recordings were obtained under visual control under the microscope. Borosilicate glass microelectrodes were used with tip resistances of 2–5 MΩ when filled with pipette solution. Action potential (AP) and sodium current recordings were measured using standard patch clamp techniques in current-clamp and voltage-clamp modes. APs were recorded at 35 °C using the whole-cell ruptured patch method, with the following bath solution (mM): NaCl 136, KCl 5.4, $CaCl_2$ 1.2, $MgCl_2{\cdot}H_2O$ 1, NaH_2PO_4 0.33, glucose 10, and HEPES 10 (pH 7.4, adjusted with NaOH). The pipette solution consisted of (mM): K-aspartate 110, KCl 20, $MgCl_2$ 1, Na_2ATP 5, HEPES 5 and EGTA 10 (pH 7.2, adjusted with KOH). Sodium currents were recorded at RT using the following bath solution were: CsCl 120, NaCl 25, $CaCl_2$ 1, $MgCl_2{\cdot}H_2O$ 1, HEPES 5, and glucose 10. Nifedipine (2.5 μM) was added before use. The pipette solution for measuring sodium currents contained: CsCl 20, CsF 110, Na_2ATP 5, HEPES 5, EGTA 5. The amplifier EPC10 was used for the recording of the electrophysiological signal. Offset potentials were nulled directly before formation of a seal. No leak subtraction was made. Fast capacitance (in pF) compensation was made after high seal was achieved; Cell capacitance (in pF) compensation was

made from whole-cell capacitance compensation after the whole-cell mode was achieved. Data were stored and analyzed with Patchmaster (v2x91) and Igor Pro (9.0).

4.10. Immunofluorescence staining

Freshly isolated hPCMs were seeded into laminin-coated confocal dishes (Bio Friend, 801002) at a density of 1×10^4 cells per group per dish. Cells were incubated for 1 h to allow adherence, and then fixed using 4 % paraformaldehyde solution (Leagene, DF0135) for 7 min at RT. Cells were rinsed 3 times with DPBS (Gibco,14287080), and blocked in blocking buffer (22.52 mg/ml glycine in PBS, 1 % BSA) for 30 min at RT. After blocking, primary antibody was added at the desired ratios in antibody dilution buffer (1 % BSA in PBS), and applied to samples overnight at 4 °C. In this study, we used a wheat germ agglutin (WGA) conjugate (Invitrogen, W11261, 1:50 dilution) and a pan sodium channel antibody (ThermoFisher, PA5-36074, 1:50 dilution). Samples were washed again with PBS for 3 times, and an Alexa Fluor 594 goat anti-rabbit IgG secondary antibody Invitrogen, A11037, 1:1000 dilution) was applied for 1 h at RT. Following 3 additional washes with PBS, DAPI was added (Invitrogen, P36981) to stain nuclei. Confocal images were obtained on a Leica SP8 Laser Confocal Microscope. Images were analyzed in ImageJ (v1.8.0) by calculating the mean fluorescence intensities per cell. At least 4 images were analyzed per group.

4.11. RNA sample preparation and real-time quantitative PCR

After hPCM isolation, 2-3 $\times 10^5$ cells were used per group for RNA extraction. 0.5 ml Trizol (ThermoFisher, 15596026) and 0.1 ml chloroform were added to cell pellets, mixed vigorously, and incubated at room temperature for 5 min. Samples were then centrifuged at12,000×*g* for 15 min at 4 °C. Following centrifugation, the aqueous phase containing RNA was transferred to a fresh tube, and isopropyl alcohol was added at a 1:1 ratio (volume), incubated for 30 min at room temperature, and centrifuged (12,000×*g*,15 min, 4 °C) again to collect RNA precipitate. The supernatant was removed, and 0.5 ml 75 % ethanol was added to wash the precipitate. The sample was vortexed, and centrifuged at 8000×*g* for 15 min at 4 °C. This washing step was repeated once, and the sample was left to air-dry. Twenty-five microliters of DEPC-treated water (Beyotime, R0021) was added per sample, and incubated at 56 °C for 15 min to redissolve RNA, after which NanoDrop2000 was used to determine RNA concentration. cDNA synthesis was performed using the iScript™ cDNA Synthesis Kit (Bio-Rad, 1708891) following the manufacturer's instructions, and reactions were run on the GeneAmp®PCR System 9700. The resulting cDNA (6 μl per sample) was mixed with 4 μl of primers, and 10 μl of iTaq Universal SYBR® Green Supermix (Bio-Rad 1725121). Real-time quantitative PCR was performed on the Applied Biosystems™ 7500 Real-Time PCR System or the QuantStudio™ 5 Real-Time PCR System. Primers used in this study are listed below.

Gene	Forward	Reverse
TNNT2	GGAGGAGTCCAAACCAAAGCC	TCAAAGTCCACTCTCTCTCCATC
MYL2	TTGGGCGAGTGAACGTGAAAA	CCGAACGTAATCAGCCTTCAG
MYL7	GCCCAACGTGGTTCTTCCAA	CTCCTCCTCTGGGACACTC
MYH6	GCCCTTTGACATTCGCACTG	GGTTTCAGCAATGACCTTGCC
MYH7	ACTGCCGAGACCGAGTATG	GCGATCCTTGAGGTTGTAGAGC
SCN5A	GCCATCTTCACAGGCGAGTGTATTG	GGGGAGAAGAAGTACTTCTGGATGATG
SCN1B	CTGCGTGGAGGTGGATTCCG	GGCTGGCTCTTCCATGAGGC
GAPDH	GAAGGTGAAGGTCGGAGTC	GCAACAATATCCACTTTACCAGAG

4.12. Western blotting

For protein extraction, 2-3 $\times 10^5$ hPCMs per group were subjected to cell lysis for 20 min in ice-cold RIPA buffer (50 mM TRIS-HCl pH 8.0, 150 mM NaCl, 0.5 % sodium deoxycholate, 0.1 % SDS, 1 % NP-40) containing Halt™ Protease and Phosphatase Inhibitor Cocktail (ThermoFisher, 1861281). Cell debris were pelleted (16,000×*g*,15 min, 4 °C), and protein concentration was determined using a BCA Protein Assay Kit (Beyotime, P0010). Sample buffer (60 mM Tris, 2 % SDS, 10 % glycerol, 0.0025 % bromophenol blue, and 3 % β-mercaptoethanol) was added to the lysate, which was then mixed and boiled at 95 °C for 5 min. Forty to 50 μg of protein per sample were loaded on SDS-PAGE gels for protein separation. Proteins were transferred onto PVDF membranes (Millipore, IPVH00010), which were then blocked with 5 % non-fat dry milk in TBST (150 mM NaCl, 20 mM Tris base, 0.1 % Tween-20) for 1 h at room temperature, washed 3 times using TBST, and incubated with corresponding primary antibodies for 24–48 h at 4 °C. Then, membranes were washed, incubated with secondary antibodies for 1 h at room temperature, washed again, and visualized using Clarity™ Western ECL Substrate (Bio-Rad, 1705069) on a ChemiDoc XRS + System (Bio-Rad). Images were analyzed with Image Lab v6.0. Primary antibodies used in this study include sodium channel pan polyclonal antibody (ThermoFisher, PA536074, 1:500 dilution), and GAPDH (Elabscience, EAB20032, 1:1000 dilution). Secondary antibodies include an anti-mouse IgG (Cell Signaling, 7076, 1:3000 dilution) and an anti-rabbit IgG (Cell Signaling, 7074, 1:3000 dilution).

4.13. Surface tension measurement

Surface tension measurements were made on a Dataphysics DCAT21 tensiometer using platinum plate method, having an accuracy

of ± 0.001 mNm^{-1}. The temperature was kept constant at 25 °C. Pure water was added into the pan to measure the surface tension, which was used for calibration of the pan and the platinum plate. After calibration, pure water removed, and 40 ml of 0.25 % MC solution was added. Calibration with pure water should be used before each determination to ensure that no sample liquid remains in the pan and the platinum plate.

4.14. Viscosity measurement

The viscosity of solutions was measured using an Anton Paar Rheometer (Physica MCR301/302) with a coaxial cylinder system. The dynamic viscoelasticity was measured with a frequency of 0.1–10 Hz at a fixed strain of 0.1 %, with a shear rate of 10–1000 s^{-1}at 37 °C. All rheological measurements were performed in the linear viscoelastic region. Thirty-one sequential measurements were taken, and the viscosity at 100 s^{-1} was used.

Data availability statement

Data included in article/supplementary material/referenced in article.

CRediT authorship contribution statement

Xun Shi: Writing – review & editing, Visualization, Validation, Resources, Investigation, Formal analysis, Data curation. **Rongjia Rao:** Validation, Resources, Formal analysis. **Miaomiao Xu:** Visualization, Validation, Software, Formal analysis. **Mengqi Dong:** Visualization, Validation, Software, Formal analysis. **Shanshan Feng:** Visualization, Validation, Software, Formal analysis. **Yafei Huang:** Validation, Formal analysis. **Bingying Zhou:** Writing – original draft, Supervision, Project administration, Methodology, Funding acquisition, Conceptualization.

Declaration of competing interest

The authors declare the following financial interests/personal relationships which may be considered as potential competing interests:Bingying Zhou reports financial support was provided by National High Level Hospital Clinical Research Funding. Bingying Zhou reports financial support was provided by National Natural Science Foundation of China. If there are other authors, they declare that they have no known competing financial interests or personal relationships that could have appeared to influence the work reported in this paper.

Acknowledgements

This work was supported by the National High Level Hospital Clinical Research Funding (grant 2022-GSP-TS-9 to B.Z.), and the National Natural Science Foundation of China (grant 82070287 to B.Z.)

Appendix A. Supplementary data

Supplementary data to this article can be found online at https://doi.org/10.1016/j.heliyon.2024.e31653.

References

[1] N. Abi-Gerges, P.E. Miller, A. Ghetti, Human heart cardiomyocytes in drug discovery and research: new opportunities in translational Sciences, Curr. Pharmaceut. Biotechnol. 21 (2020) 787–806, https://doi.org/10.2174/1389201021666191210142023.
[2] L. Pang, P. Sager, X. Yang, H. Shi, F. Sannajust, M. Brock, J.C. Wu, N. Abi-Gerges, B. Lyn-Cook, B.R. Berridge, N. Stockbridge, Workshop report: FDA workshop on improving cardiotoxicity assessment with human-relevant platforms, Circ. Res. 125 (2019) 855–867, https://doi.org/10.1161/CIRCRESAHA.119.315378.
[3] N. Nguyen, W. Nguyen, B. Nguyenton, P. Ratchada, G. Page, P.E. Miller, A. Ghetti, N. Abi-Gerges, Adult human primary cardiomyocyte-based model for the simultaneous prediction of drug-induced inotropic and pro-arrhythmia risk, Front. Physiol. 8 (2017) 1073, https://doi.org/10.3389/fphys.2017.01073.
[4] X. Tang, H. Liu, R. Rao, Y. Huang, M. Dong, M. Xu, S. Feng, X. Shi, L. Wang, Z. Wang, B. Zhou, Modeling drug-induced mitochondrial toxicity with human primary cardiomyocytes, Sci. China Life Sci. (2023), https://doi.org/10.1007/s11427-023-2369-3.
[5] L. Wang, P. Yu, B. Zhou, J. Song, Z. Li, M. Zhang, G. Guo, Y. Wang, X. Chen, L. Han, S. Hu, Single-cell reconstruction of the adult human heart during heart failure and recovery reveals the cellular landscape underlying cardiac function, Nat. Cell Biol. 22 (2020) 108–119, https://doi.org/10.1038/s41556-019-0446-7.
[6] B. Zhou, X. Shi, X. Tang, Q. Zhao, L. Wang, F. Yao, Y. Hou, X. Wang, W. Feng, L. Wang, X. Sun, L. Wang, S. Hu, Functional isolation, culture and cryopreservation of adult human primary cardiomyocytes, Signal Transduct. Targeted Ther. 7 (2022) 254, https://doi.org/10.1038/s41392-022-01044-5.
[7] A. Blaeser, D.F. Duarte Campos, U. Puster, W. Richtering, M.M. Stevens, H. Fischer, Controlling shear stress in 3D bioprinting is a key factor to balance printing resolution and stem cell integrity, Adv. Healthcare Mater. 5 (2016) 326–333, https://doi.org/10.1002/adhm.201500677.
[8] Y. Huang, X. Jia, K. Bai, X. Gong, Y. Fan, Effect of fluid shear stress on cardiomyogenic differentiation of rat bone marrow mesenchymal stem cells, Arch. Med. Res. 41 (2010) 497–505, https://doi.org/10.1016/j.arcmed.2010.10.002.
[9] J.D. Michaels, E.T. Papoutsakis, Polyvinyl alcohol and polyethylene glycol as protectants against fluid-mechanical injury of freely-suspended animal cells (CRL 8018), J. Biotechnol. 19 (1991) 241–257, https://doi.org/10.1016/0168-1656(91)90062-z.

[10] C.L. McDowell, R.T. Carver, E.T. Papoutsakis, Effects of methocel A15LV, polyethylene glycol, and polyvinyl alcohol on CD13 and CD33 receptor surface content and metabolism of HL60 cells cultured in stirred tank bioreactors, Biotechnol. Bioeng. 60 (1998) 251–258, https://doi.org/10.1002/(sici)1097-0290(19981020)60:2<251::aid-bit12>3.0.co;2-p.
[11] E.T. Papoutsakis, Media additives for protecting freely suspended animal cells against agitation and aeration damage, Trends Biotechnol. 9 (1991) 316–324, https://doi.org/10.1016/0167-7799(91)90102-n.
[12] S. Goldblum, Y.K. Bae, W.F. Hink, J. Chalmers, Protective effect of methylcellulose and other polymers on insect cells subjected to laminar shear stress, Biotechnol. Prog. 6 (1990) 383–390, https://doi.org/10.1021/bp00005a011.
[13] M.S. Croughan, E.S. Sayre, D.I. Wang, Viscous reduction of turbulent damage in animal cell culture, Biotechnol. Bioeng. 33 (1989) 862–872, https://doi.org/10.1002/bit.260330710.
[14] M.C. Borys, E.T. Papoutsakis, Formation of bridges and large cellular clumps in CHO-cell microcarrier cultures: effects of agitation, dimethyl sulfoxide and calf serum, Cytotechnology 8 (1992) 237–248, https://doi.org/10.1007/BF02522041.
[15] Y. Chisti, Animal-cell damage in sparged bioreactors, Trends Biotechnol. 18 (2000) 420–432, https://doi.org/10.1016/s0167-7799(00)01474-8.
[16] D. Chattopadhyay, J.F. Rathman, J.J. Chalmers, The protective effect of specific medium additives with respect to bubble rupture, Biotechnol. Bioeng. 45 (1995) 473–480, https://doi.org/10.1002/bit.260450603.
[17] A.M. Gerdes, J.M. Capasso, Structural remodeling and mechanical dysfunction of cardiac myocytes in heart failure, J. Mol. Cell. Cardiol. 27 (1995) 849–856, https://doi.org/10.1016/0022-2828(95)90000-4.
[18] R.C. Rowe, The molecular weight of methyl cellulose used in pharmaceutical formulation, Int. J. Pharm. 11 (1982) 175–179, https://doi.org/10.1016/0378-5173(82)90054-0.
[19] B. Sasa, P. Odon, S. Stane, K. Julijana, Analysis of surface properties of cellulose ethers and drug release from their matrix tablets, Eur. J. Pharmaceut. Sci. 27 (2006) 375–383, https://doi.org/10.1016/j.ejps.2005.11.009.
[20] D. Wu, J. Cheng, X. Su, Y. Feng, Hydrophilic modification of methylcellulose to obtain thermoviscosifying polymers without macro-phase separation, Carbohydr. Polym. 260 (2021) 117792, https://doi.org/10.1016/j.carbpol.2021.117792.
[21] T.D.a.K. Karan, Binders in wet granulation, in: S.I.F.B. Ajit S. Narang (Ed.), Handbook of Pharmaceutical Wet Granulation, ACADEMIC PRESS, 2019, pp. 317–349, https://doi.org/10.1016/C2016-0-00287-5.
[22] Methocel Cellulose Ethers, Technical Handbook, 2015. https://www.iff.com/portfolio/markets/food-beverage/hydrocolloids-texturants-cellulosics.
[23] Methylcellulose, Methylhydroxypropycellulose, Hypromellose, Physical and Chemical Properties, 2015. http://www.brenntagspecialties.com/en/downloads/Products/Multi_Market_Principals/Aqualon/Benecel_Brochure.pdf.
[24] L. Bonetti, L. De Nardo, S. Fare, Thermo-responsive methylcellulose hydrogels: from design to applications as smart biomaterials, Tissue Eng., Part B 27 (2021) 486–513, https://doi.org/10.1089/ten.TEB.2020.0202.
[25] M.M. Salzman, J.A. Bartos, D. Yannopoulos, M.L. Riess, Poloxamer 188 protects isolated adult mouse cardiomyocytes from reoxygenation injury, Pharmacol Res Perspect 8 (2020) e00639, https://doi.org/10.1002/prp2.639.
[26] J.G. Moloughney, N. Weisleder, Poloxamer 188 (p188) as a membrane resealing reagent in biomedical applications, Recent Pat. Biotechnol. 6 (2012) 200–211, https://doi.org/10.2174/1872208311206030200.
[27] B. Wittgren, M. Stefansson, B. Porsch, Interactions between sodium dodecyl sulphate and non-ionic cellulose derivatives studied by size exclusion chromatography with online multi-angle light scattering and refractometric detection, J. Chromatogr. A 1082 (2005) 166–175, https://doi.org/10.1016/j.chroma.2005.05.047.